Title
Utilization of Recently Enhanced Simulation Tools and Empirical Ground Motion Databases to Improve Ground Motion Prediction Capabilities

Author
Khodavirdi, Khatereh

Publication Date
2013

Peer reviewed|Thesis/dissertation

University of California

Los Angeles

Utilization of Recently Enhanced Simulation Tools and Empirical Ground Motion Databases to Improve Ground Motion Prediction Capabilities

A thesis submitted in partial satisfaction

of the requirements for the degree

Master of Science in Statistics

by

Khatereh Khodaverdi

2013

Abstract of the Thesis

Utilization of Recently Enhanced Simulation Tools and Empirical Ground Motion Databases to Improve Ground Motion Prediction Capabilities

by

Khatereh Khodaverdi

Master of Science in Statistics

University of California, Los Angeles, 2013

Professor Rick Paik Schoenberg, Chair

My research was strongly influenced by ongoing Next Generation Attenuation projects (NGA), which is sponsored by Pacific Earthquake Engineering Research Center (PEER). This far, PEER has sponsored two landmark national projects for developing NGA relationship in active tectonic regions. The result of these two projects will be incorporated into national hazard maps developed by United States Geological Survey (USGS). However, since the national seismic hazard maps include stable continental regions and subduction zones, it is desired to extend those studies to other tectonic regions. NGA-Subduction project has recently been initiated to address Subduction Zones (SZ).

For this project, I collaborated with PEER researcher for processing the data of main shock recordings of the Tohoku earthquake. I also analyzed the data to evaluate the implications of this data set with respect to magnitude-, distance-, and site-scaling in existing GMPEs for SZs. The $M_w = 9.0$ Tohoku-oki Japan earthquake produced approximately 2000 ground motion recordings. We consider 1238 three-component accelerograms corrected with component-specific low-cut filters. The recordings have rupture distances between 44 and 1000 km, time-

averaged shear wave velocities of $V_{s30} = 90$ to $1900\,\mathrm{m\,s^{-1}}$, and usable response spectral periods of 0.01 to $> 10\,\mathrm{s}$. The data support the notion that the increase of ground motions with magnitude saturates at large magnitudes. High frequency ground motions demonstrate faster attenuation with distance in backarc than in forearc regions, which is only captured by one of the four considered ground motion prediction equations for subduction earthquakes. Recordings within 100 km of the fault are used to estimate event terms, which are generally positive (indicating model under-prediction) at short periods and zero or negative (over-prediction) at long periods. We find site amplification to scale minimally with V_{s30} at high frequencies, in contrast with other active tectonic regions, but to scale strongly with V_{s30} at low frequencies.

It is envisioned that the research outlined herein could help earthquake engineering community to design infrastructures which are more resistant to earthquakes by improving ground motion prediction capabilities.

The thesis of Khatereh Khodaverdi is approved.

Qing Zhou

Mark S. Handcock

Rick Paik Schoenberg, Committee Chair

University of California, Los Angeles

2013

Table of Contents

List of Figures

List of Tables

Acknowledgments

This thesis would not have been possible without the help of many wonderful people with whom I have had the pleasure to work. First and foremost, I would like to thank my academic advisor, Professor Rick Paik Schoenberg. Thank you for providing me with the necessary confidence in my abilities and pushing me to exceed what I thought were my limitations. Rick has been a great mentor and provided in numerous occasions incredibly insightful suggestions that helped me look at problems under a different light. Prof. Handcock has been a persistent reminder of the value of perfection. Throughout exciting discussions and his insights, he has instilled into me a commitment to careful critical thinking and a love for data. I would like to thank Prof. Zhou for all his support from the very beginning of taking classes in statistics department at UCLA.

CHAPTER 1

Introduction

1.1 Context and Applications of Ground Motion Prediction

Recent earthquakes in Japan and New Zealand provide vivid reminders of the threats posed to infrastructure and population centers from seismic activity. While earthquakes occur along plate boundaries world-wideon a regular basis, the extent of damage and life loss depends largely on the severity of the ground shaking and the proximity of strong shaking and secondary effects (e.g., ground failure) to population centers. The severity of shaking, in turn, depends principally on magnitude, proximity to source, and local site conditions. Ground motions are parameterized for use in engineering design through intensity measures (IMs) that characterize ground motion amplitude, frequency content, duration, or combinations of those attributes. The mostly commonly used IMs are 5% damped pseudo spectral acceleration over a range of periods typically spanning from zero (PGA) to about 10 s.

Probabilistic seismic hazard analysis (PSHA) is the process of computing the probable rate of exceedanceof various levels of IMs at a site by considering all possible earthquakes and the distribution of IMs resulting from those earthquakes, along with the relative likelihoods of each combination.This process is illustrated in Figure 1.1, which is adapted from Cornell (1968) [Cor68]. PSHA provides IM values with a specified probability of occurrence in a given time period, which

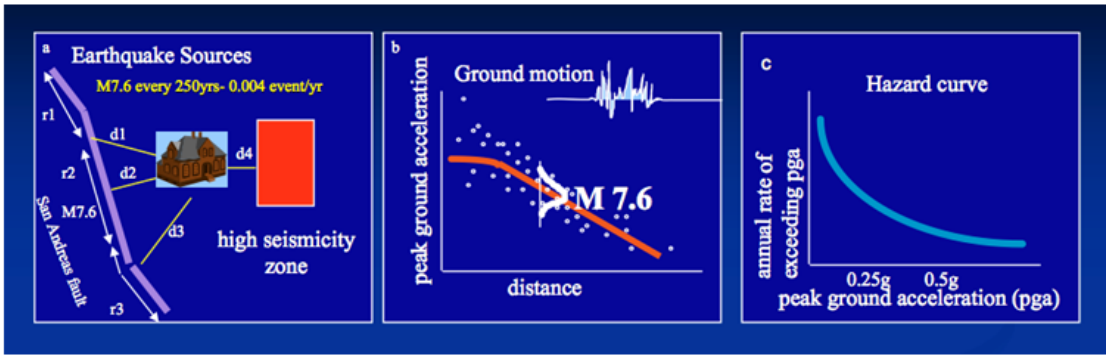

Figure 1.1: Probabilistic seismic hazard analysis methodology. (Source: `http://earthquake.usgs.gov/hazards/about/workshops/thailand/downloads/Thailand-workshop pshatraining1-new-.pdf`)

facilitates rational engineering design of structures that is based on community consensus level of seismic risk. Both traditional code-based design approaches and performance-based earthquake engineering methodologies utilize PSHA as the basis for demand specification.

As illustrated in part (a) of Figure 1.1, the first step in calculating the hazard curve determine magnitude, and distance and rate of earthquakes on fault zones. Part (b) of Figure 1.1 shows the second step of the framework, which is calculation of ground motion distribution for that magnitude and that distance. The last step consists of summing the product of annual rate of earthquake and probability that earthquake will exceed certain ground motion level. The summation will go over the rates for all earthquakes in the model at each ground motion to get a hazard curve.

As illustrated in part (b) of Figure 1.1, a critical component of PSHA is the prediction of ground motion IMs conditional on magnitude, distance, and site parameters. This is done with semi-empirical models known as ground motion prediction equations (GMPEs). GMPEs incorporate expressions that represent the scaling of IMs with magnitude, distance, and site parameters. Distance is typically represented with the closest distance to the rupture surface (R_{rup}) or

the closest distance to the surface projection of the rupture surface (R_{jb}). Site condition is represented either with discrete site categories (e.g., rock and soil) or with the time-averaged shear wave velocity in the upper 30 m (V_{s30}) of the site.

Ground motion characteristics conditional on magnitude, distance, and site condition, are known to exhibit broad regional variations for the different tectonic regimes that occur around the world. There are four basic tectonic categories of interest for the study of ground motion characteristics, as follows:

1. Stable continental regions (SCRs) located away from plate boundaries (e.g., central and eastern north America)

2. Subduction zone (SZ) plate boundaries, in which seismicity occurs at the interface between plates (inter-face events) and within the subducting or over-riding slabs (intra-slab events). Examples include Chile, Japan, and the Pacific northwest portion of the US.

3. Active crustal regions (ACRs) located near plate boundaries, such as California, New Zealand, Turkey, and Iran.

4. Volcanic regions, which typically are in active crustal or subduction regions, but are differentiated for ground motion prediction because of the relatively small event magnitudes and different crustal properties.

The Pacific Earthquake Engineering Research Center (PEER) has played a leading role in the development of GMPEs for ACRs and SCRs. The work on ACRs includes the landmark Next Generation Attenuation (NGA) project (Power et al., 2008) [PCA08] that produced five GMPEs that have seen wide use worldwide. The NGA project is in the process of being updated as part of the NGA-West2 project (`http://peer.berkeley.edu/ngawest2/`), which is nearing completion. Both the NGA and NGA-West2 projects utilize large empirical data sets to guide the evaluation of GMPEs through rigorous regression procedures.

Despite the large size of the data sets, there remain conditions for which data is sparse, and yet the GMPE must be able to provide ground motion estimates for PSHA applications. These conditions include long-period ground motions, large magnitude conditions, and site conditions at the limits of the typical ranges (i.e., very soft soils, very firm bedrock). Due to the lack of data for such conditions, the available models can have significant variability due to lack of knowledge, which is known as epistemic uncertainty. In many cases, the models are influenced by the results of ground motion simulations that can help to fill in data gaps.

PEER has sponsored many public events to present the results of the NGA and NGA-West2 projects to the earthquake engineering community. The results of these studies will be incorporated into future versions of national seismic hazard maps by the USGS that are used in building codes. However, since the national seismic hazard maps include SCR and SZ regions in addition to ACRs, NGA projects are currently only impacting the maps for a portion of the US. It is desired to extend this reach to the remainder of the country due to the strong scientific basis and consensus building process associated with NGA project. For this reason, NGA-Subduction project has recently been initiated to address SZ regions.

This thesis will focus to contribute to subduction zone earthquakes. SZs provide a major contribution to seismic hazards in many regions of the world, but the available GMPEs are highly variable with respect to critical issues such as the regionalization of their data sets and the parameterization of site effects (i.e., most use site categories, whereas in the more contemporary models for ACRs V_{s30} has been adopted). Moreover, major interface subduction zone events (2010 Maule Chile and 2011 Tohoku Japan) have provided extremely valuable data near the upper end of the magnitude range applicable for SZs, which will significantly benefit the next-generation of SZ GMPEs.

The first phase of NGA-subduction is collection and processing of recorded

data from previous subduction earthquakes such as Tohoku, Japan earthquake (M_w = 9.0, March 2011). The writer was involved during the summer of 2012 to process the main shock recordings of the Tohoku earthquake and convert the processed records to the PEER flat file format. I then performed analyses to evaluate the implications of this data set with respect to magnitude-, distance, and site-scaling in existing GMPEs for SZs. The findings and analysis are presented in this writings.

This thesis will try to address the gaps in current knowledge discussed above by contributing to the national projects in this field. The findings were also presented as a journal paper in earthquake spectra [SMG13].

1.2 Motivation

On March 11, 2011, the largest earthquake in Japan's recent history hit Tohoku. The M_w = 9.0 event produced strong shaking, a devastating tsunami, and substantial infrastructure damage. The event is the largest magnitude earthquake to produce strong motion recordings, and there are over 2000 three-component records.

I visited PEER in summer of 2012 to assist in processing the main-shock and aftershock recordings of the 2011 Tohoku earthquake. This process included identification of those records where the data quality seemed questionable. For example, some records appeared to only include the S-wave component and were excluded.

I then undertook residuals analysis of the main shock data to investigate the implications of the event for magnitude-scaling, distance-scaling, and site-scaling in interface subduction zone earthquakes. This work was presented in the rest of this writing.

1.3 Problem Statement

The $M_w = 9.0$ Tohoku-oki earthquake occurred on March 11, 2011 off the Pacific Coast of Japan. This earthquake is associated with the subduction process of the Pacific plate beneath the North American (continental) plate at the Japan Trench, which occurs with a convergence rate of about 8–9 cm/yr. The earthquake resulted from thrust-faulting at the interface between the two plates, which have produced many large historic earthquakes including the 1896 Meiji-Sanriku earthquake (estimated $M_w = 8.5$) and nine events of magnitude seven or greater in the modern instrumental era (since 1973, when the Japan Meteorological Agency has distributed relatively high quality seismic data) including the 1978 earthquake ($M_w = 7.4$). USGS (2012) placed the mainshock hypocenter about 129 km east of Sendai (38.297° N, 142.372° E) at a depth of 30 km (USGS, 2012). The rupture length (along strike) extended for approximately 480 km from the north end of Honshu Island to Tokyo Bay in the south and had a down-dip width of approximately 180 km. The event produced a destructive tsunami devastating coastal areas including catastrophic damage at the Fukushima nuclear power plant, extensive ground failure from liquefaction and slope instability, and surprisingly modest shaking-related damage as described in other papers in this Special Issue.

The Tohoku earthquake is the largest magnitude event to have produced strong motion recordings. Figure 1.2 shows the strong motion data distribution for worldwide subduction zone interface earthquakes through 2011. The data shown in Figure 1.2 are from the dataset used by Atkinson and Boore (2003) [AB03], supplemented with the more recent events listed in the legend and caption. The general characteristics of the ground motions from this major event have been described previously by Furumura et al. (2011) [FTN11], Skarlatoudis and Papazachos (2012) [SP12], and Midorikawa et al. (2012) [MMA12]. In the present work, we extend the previous studies by performing more quantitative residuals

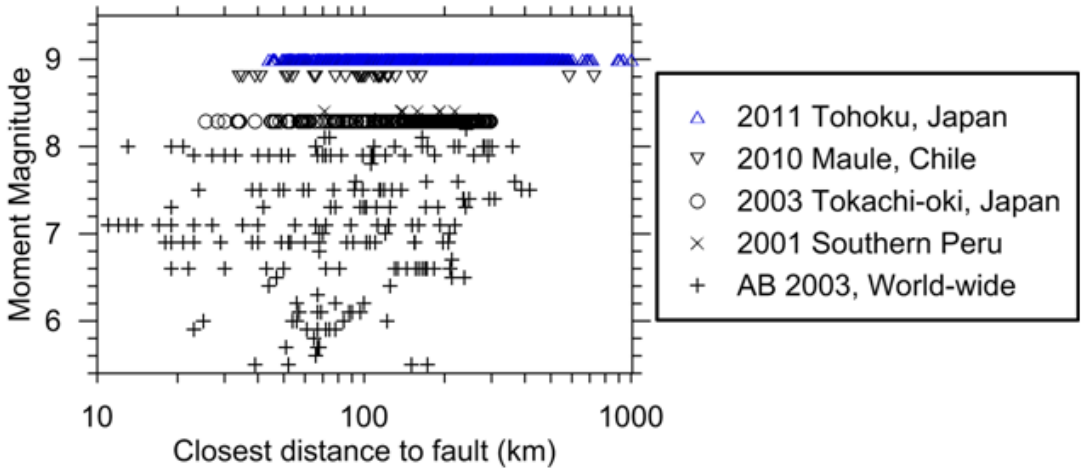

Figure 1.2: Distribution of strong motion data for interface subduction zone earthquakes. Data taken from electronic supplement to Atkinson and Boore (2003) [AB03] for data prior to 2001, Rodriguez-Marek et al. (2010) [RBP10] for 2001 Southern Peru earthquake, J. Zhao (pers. communication, 2011) for the 2003 Tokachi-oki earthquake, and Boroschek et al. (2012) [BCK12] for the Maule earthquake.

analysis to investigate event terms, distance attenuation trends, and site effects.

1.4 Organization of this writing

In the rest of this writing, we begin by describing the ground motion database including the record processing procedures that were applied and the evaluation of site conditions from available data resources. We then compare observed spectral accelerations to predictions from four ground motion prediction equations (GMPEs), three of which are international models for subduction zone earthquakes, and one of which is Japan-specific. We formally examine issues related to magnitude-scaling, distance-scaling, site effects, and within-event data dispersion. These results will be directly applicable to the development of next-generation GMPEs for interface subduction zone earthquakes. Analyses of this type have

not been performed previously on the Tohoku data set, although where related prior work has been performed (e.g., on the distance attenuation issue), we compare our results to those described previously.

CHAPTER 2

Ground Motion Database

2.1 Ground motion networks

As described by Midorikawa et al. (2012) [MMA12], research ground motion networks that recorded the Tohoku-oki mainshock include the K-net and Kik-net maintained by the National Research Institute for Earth Science and Disaster Prevention (NIED), PARI-net operated by the Port and Airport Research Institute, and BRI-net operated by the Building Research Institute. Additional networks used for disaster management include the JMA-net operated by the Japan Meteorological Agency, various prefectures networks, and an MLIT network operated by the Ministry of Land, Infrastructure, and Transport.

In the present study, we utilized available data from the K-net, Kik-net, PARI-net, and JMA-net arrays. The available data were reviewed to identify through visual inspection recordings for which all three components demonstrated a clear onset of shaking, so as to exclude from the data set records that may have had a P-trigger. This process yielded 1238 triaxial accelerographs. Further information on ground motion networks in Japan and recorded data from the Tohoku-oki mainshock are provided by Midorikawa et al. (2012) [MMA12].

2.2 Data processing

A total of 1238 three-component uncorrected digital accelerograms were selected as described above. Sponsored by the Pacific Earthquake Engineering Research Center (PEER), those motions were processed by Pacific Engineering and Analysis following PEER/NGA protocols (Darragh et al., 2004 [DSG04]; Chiou et al., 2008 [CDD08]), which include selection of record-specific corner frequencies to optimize the usable frequency range. For Kik-net sites, only data from the ground surface stations are considered. The most important filter applied to the data is the low-cut filter, which removes low frequency noise effects. We take the minimum usable frequency as $1.25 \times f_{HP}$, where f_{HP} is the high-pass (equivalent to low-cut) corner frequency used in the processing. Using the filtered records, we computed the intensity measures of peak acceleration (PGA), peak velocity (PGV), and pseudo acceleration response spectra at a range of periods between 0.01 s and 10.0 s. Figure 2.1 presents the number of usable recordings as a function of period. A usable recording for period T is defined as having both horizontal components with $T < 1/\left(1.25 f_{HP}\right)$. The data set is seen to fall off for periods beyond about 20 s to 30 s.

2.3 Site conditions

The NIED web site contains shear- and compression-wave velocity profiles for each of the K-net and Kik-net sites except for five ocean-bottom sites. Kik-net profiles are always deeper than 30 m, whereas K-net profiles are always 20 m or shallower. The measured shear wave velocity profiles were used to compute V_{s30} as follows:

1. When profile depth (z_p) is 30 m or greater (Kik-net sites), the Vs profile is used to compute V_{s30} as the ratio of 30 m to the shear wave travel time above a depth of 30 m.

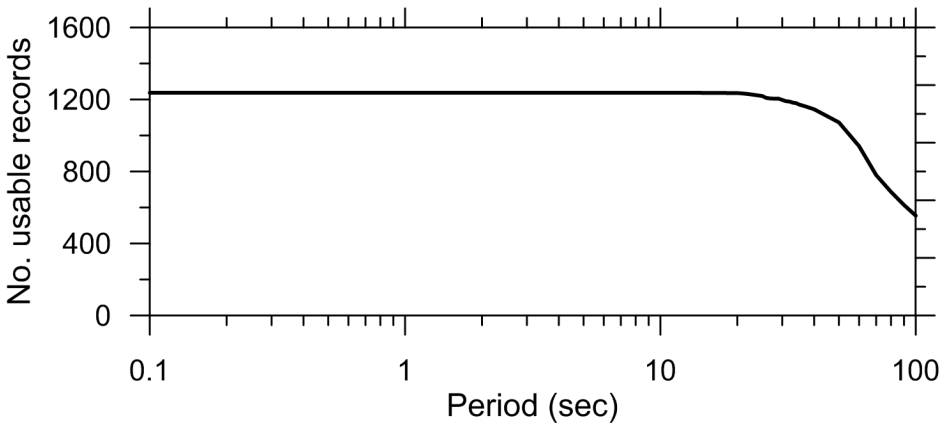

Figure 2.1: Number of usable two-component horizontal records as function of spectral period for the data set considered in this study. At this time, no records were processed to be usable beyond 5.0 s, although subsequent more detailed processing will likely yield a substantial number of records that are usable at low frequencies.

2. When $z_p < 30\,\mathrm{m}$, compute V_{sz} as the ratio of z_p to shear wave travel time from z_p to the ground surface.

3. When $z_p = 20\,\mathrm{m}$, compute V_{s30} from V_{sz} and z_p using the correlation relationships originally developed for California by Boore (2004) [Boo04]. When $z_p \leq 10\,\mathrm{m}$, compute V_{s30} from V_{sz} and z_p using the correlation relationships developed from Kik-net data by Boore et al. (2011) [BTC11]. For intermediate depths of $10 < z_p < 20\,\mathrm{m}$, interpolate between the above values.

The rationale behind Step (3) above is that shallow-depth K-net profiles likely encountered firm geologic materials causing borehole drilling to stop. Firm geologic conditions are also common for Kik-net sites. On the other hand, 20 m K-net profiles are likely deeper sediments similar to the conditions prevalent in California. A histogram of V_{s30} values in the data set is shown in Figure 2.2. No velocity profiles are available for the five ocean-bottom sites and V_{s30} was assumed as $180\,\mathrm{m\,s^{-1}}$ for the present study.

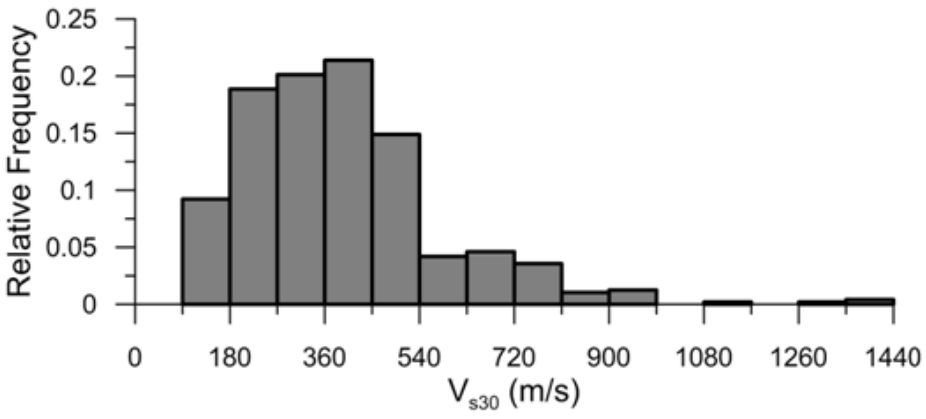

Figure 2.2: Histogram of V_{s30} values in dataset.

For sites without velocity profiles, which includes most of the JMA-net and about half of the PARI-net sites, we estimate V_{s30} using a proxy-based method described by Matsuoka et al. (2006) [MWF06]. This method uses geomorphic and geologic conditions mapped across Japan (Wakamatsu and Matsuoka, 2008) [WM08] that are correlated by category to V_{s30}.

CHAPTER 3

Comparisons to GMPEs

In this section we compare the Tohoku-oki earthquake mainshock data described in the previous section to several GMPEs using an approach, originally presented by Scasserra et al. (2009) [SSB09], in which specific attributes of the GMPE are examined relative to the data. In particular, we investigate the implications of the data for magnitude scaling, distance scaling, intra-event dispersion, and site effects. An alternative approach was presented by Scherbaum et al. (2004) [SCS04], in which overall goodness of fit of data to a model is computed by comparing normalized residuals to the standard normal variate. The selected approach was used because we seek the aforementioned physical insights provided by the ground motion data.

3.1 Applicable models

We utilize ground motion prediction equations (GMPEs) for interface subduction zone earthquakes by Atkinson and Boore (2003, 2008) [AB03, AB08], Abrahamson et al. (2012), [ANA12] and Zhao et al. (2006), [ZZA06] which we refer to subsequently as AB 2003, AEA 2012, and ZEA 2006, respectively. The first and third of these GMPEs were used to predict subduction zone ground motions in the USGS seismic hazard maps (Petersen et al. 2008) [PFH08]. The AEA 2012 model has been identified for use in subsequent versions of the USGS maps. We also consider a Japan-specific model by Si and Midorikawa (2000) [SM00] that utilizes Japanese data from crustal, inter-plate, and intra-plate events. That model,

which applies to PGA and PGV only, was selected due to its widespread usage in Japan and is denoted SM 2000.

AB 2003 is based on world-wide subduction zone data and includes models specific to various regions of the world, including South America and Japan. The generic, non-regional version of the model is used here and the event terms are subsequently used to check the AB 2003 regional correction for Japan. We recognize that Atkinson and Macias (2009) [AM09] have developed a subsequent GMPE for subduction regions, derived in part from simulations of large subduction earthquakes, which they recommend over AB 2003. The original AB 2003 model was selected due to its usage in numerous engineering applications (Petersen et al., 2008 [PFH08]; Stewart et al. 2012 [SSB12]). The largest magnitude in the AB data set is 8.3 and the largest well-recorded event is 8.0. ZEA 2006 and SM 2000 utilize data from world-wide crustal events, and they use Japanese data from multiple source types including interface and intraslab subduction zone earthquakes. The AB and ZEA models apply to the geometric mean of the two horizontal components, whereas SM 2000 applies to the larger of two horizontal components. The developers of the AB, SM, and ZEA models each indicated their equations as applicable to an upper bound magnitude of 8.3. The AEA model is considered to be applicable to magnitude 9.0.

3.2 Magnitude scaling of spectral ordinates

A key issue in ground motion prediction for interface subduction zone earthquakes is the functional form used for magnitude scaling. Many models produce essentially linear scaling of the logarithm of ground motion with magnitude (e.g., SM model in Figure 3.1 and a linear form of ZEA that is not used here), whereas others apply higher order terms that produce saturation of ground motion with increasing magnitude (e.g., AB 2003 and AEA 2012 models, as well as quadratic

form of ZEA 2006 model in Figure 3.1. The SM 2000 model predictions shown in Figure 3.1 and elsewhere have been divided by 1.1 to correct from largest horizontal component to the geometric mean, based on the recommendations of Beyer and Bommer (2006) [BB06].

In Figure 3.1 we plot ground motion intensity measures (IMs) at several spectral periods versus magnitude. The data are from AB 2003 (database available through an electronic supplement), the 2001 Southern Peru earthquake (Rodriguez-Marek et al., 2010) [RBP10], the Maule, Chile, earthquake (Boroschek et al., 2012) [BCK12], and Tohoku-oki earthquake. The data plotted have rupture distances between 70 km and 150 km and include all site conditions. The GMPE medians are for a distance of 100 km and an average site condition corresponding to $V_{s30} = 300\,\mathrm{m\,s^{-1}}$. The data for the Maule and Tohoku events appears to support saturation of ground motions at large magnitudes for the IMs considered, especially for high frequency IMs.

3.3 Distance scaling and residuals analysis

Figure 3.2 shows RotD50 values (similar to geometric mean; Boore, 2010 [Boo10]) PGA, 0.1 s, 1.0 s, and 3.0 s pseudo spectral accelerations (PSa) at 5% damping versus rupture distance. Data are shown for the following bins of V_{s30} :$< 200\,\mathrm{m\,s^{-1}}$, 200–400 $\mathrm{m\,s^{-1}}$, 400–760 $\mathrm{m\,s^{-1}}$, and $> 760\,\mathrm{m\,s^{-1}}$. Also shown in Figure 3.2 are medians (μ) and medians $\pm$ one intra-event standard deviation (σ_{ln}) for the ZEA 2006 GMPE and medians for AB 2003 (without regional correction for Japan), AEA 2012 (for forearc and backarc regions) and SM 2000 (PGA only). The GMPEs are plotted for site categories corresponding to a reference condition of $V_{s30} = 300\,\mathrm{m\,s^{-1}}$. All of the GMPEs except AEA 2012 were extrapolated beyond the reported maximum usable magnitude for the present application.

Several significant trends are evident from Figure 3.2. First, we see that the

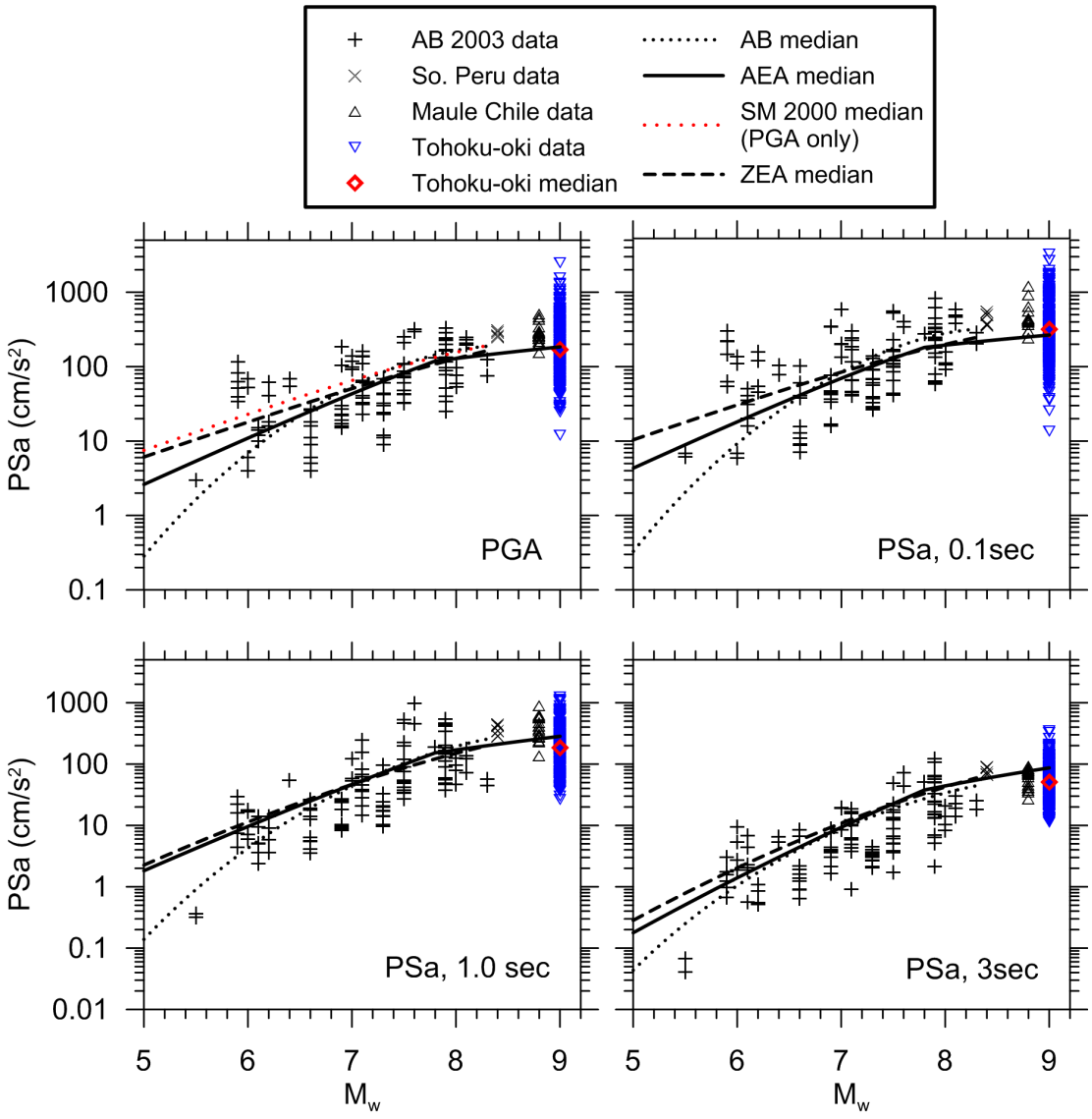

Figure 3.1: Scaling of spectral ordinates and PGA with magnitude from AB 2003 data set as well as Southern Peru, Maule (Chile) and Tohoku-oki earthquake data for distances between 70 km and 150 km. Median predictions from three GMPEs shown, which apply for reference soil conditions (approximate $V_{s30} = 300\,\mathrm{m\,s^{-1}}$) and distance of 100 km.

ZEA 2006, SM 2000, and AEA 2012 GMPEs have faster distance attenuation rates than AB 2003, and in addition, the data consistently attenuate faster with distance than predicted by AB 2003. ZEA 2006 appears to capture the distance attenuation rate at the two longer considered periods (1.0 s and 3.0 s), but it cannot capture the relatively fast attenuation of high frequency parameters (0.1 s PSa and PGA) beyond about 100 km. The SM 2000 trend for PGA is nearly identical to that of ZEA 2006. Average site effects are also evident from the data in Figure 3.2; soil sites (green and blue dots) are clearly higher on average than rock sites (purple and red dots) at the longer periods, but this trend does not hold for PGA or 0.1 s PSa. Site effects are analyzed more formally in the following section.

Figure 3.3 shows the data from Figure 3.2 segregated into forearc and backarc regions according to the boundary in Figure 2.1. Data are shown only for intermediate site classes having V_{s30} = 200–760 m s^{-1}. The break in slope that occurs in the high frequency data near R_{rup} = 100–200 km is seen to be the consequence of a transition from predominantly forearc to backarc sites. The relatively rapid attenuation in backarc regions is thought to result from increased anelastic attenuation (Ghofrani and Atkinson, 2011) [GA11]. AEA 2012 is the only GMPE that incorporates the slope break associated with the forearc to backarc transition, and the backarc model does provide an improved fit, especially at short periods.

To more accurately evaluate the performance of the GMPEs, including corrections for site effects, we calculate total residuals (including inter- and intra-event components; see, for example, Scasserra et al. (2009) [SSB09] for further explanation of the methodology) for each data point considering the appropriate source distance and site condition as follows:

$$R_i = \ln\left(IM_i\right)_{rec} - \ln\left(\mu_i\right)_{GMPE} \tag{3.1}$$

where $\left(IM_i\right)_{rec}$ = value of ground motion intensity measure from recording i and

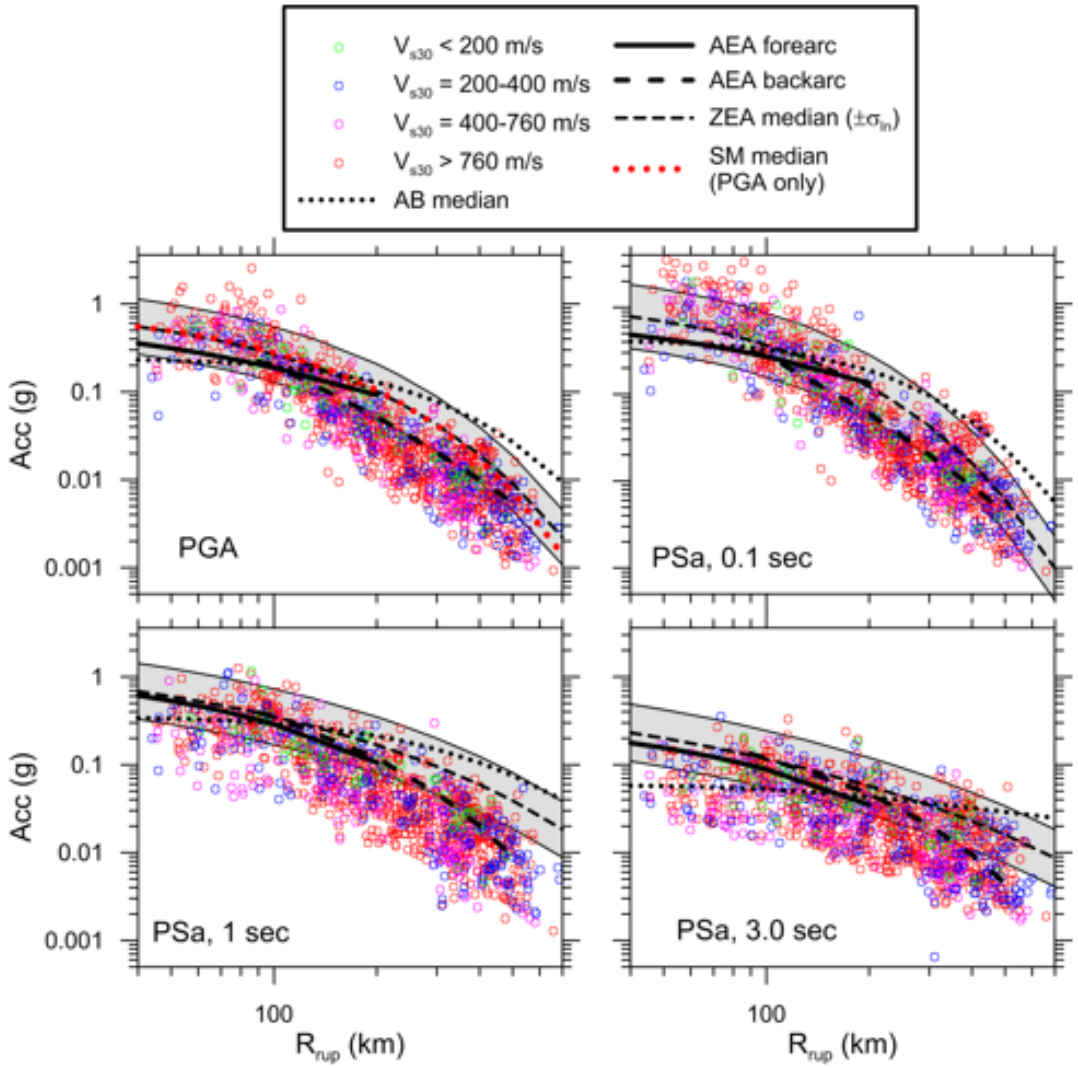

Figure 3.2: Attenuation of PGA and spectral accelerations with distance and comparison to GMPEs for reference condition equivalent to $V_{s30} = 300\,\mathrm{m\,s^{-1}}$. For ZEA 2006 both the median (μ) and median one standard deviation ($\mu \pm \sigma_{ln}$) are shown, whereas for AB 2003, AEA 2012, and SM 2000 only medians are shown. The data are plotted as geometric means. ZEA 2006 applies to the geometric mean. AB 2003 applies to random component and no correction to the AB 2003 median has been applied. The SM 2000 median is divided by 1.1 to adjust from larger component to geometric mean per the recommendations of Beyer and Bommer (2006) [BB06].

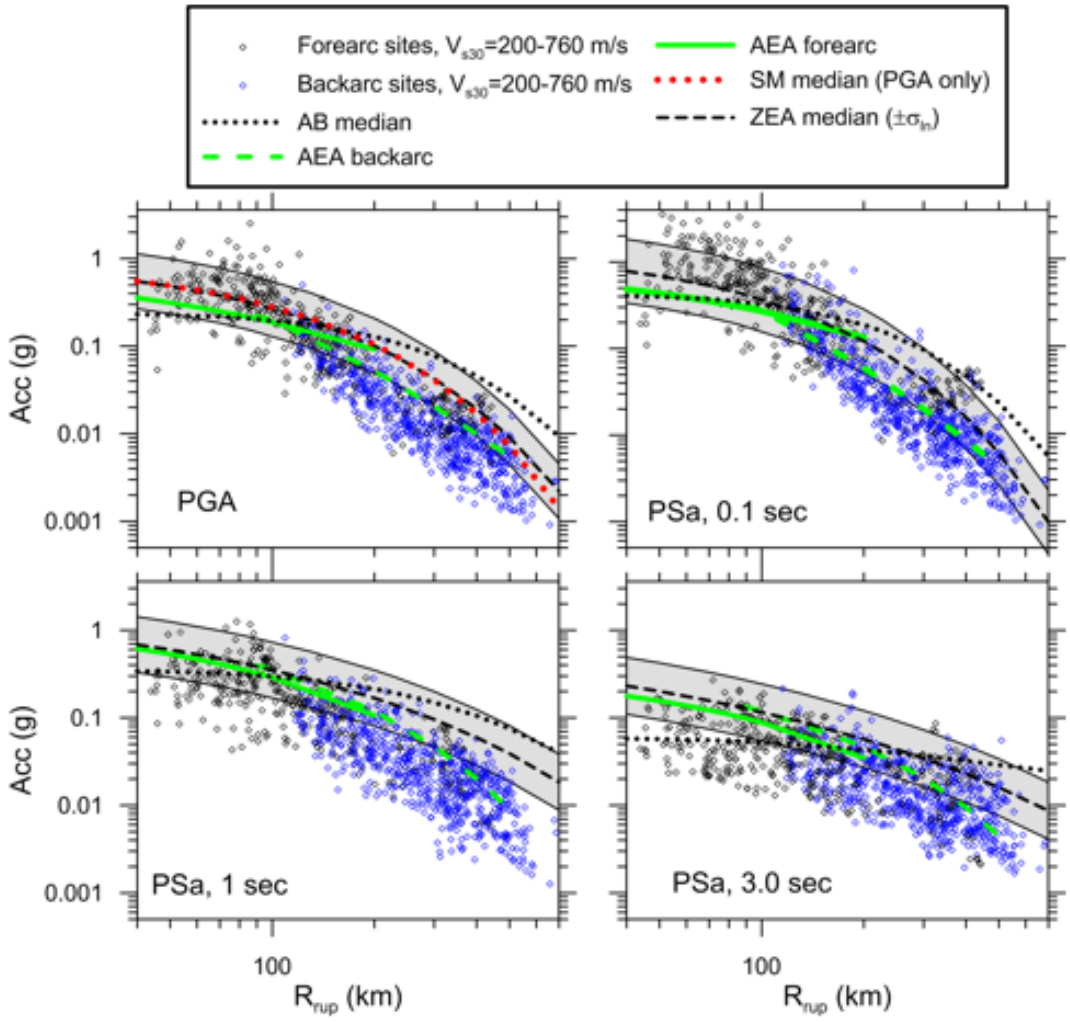

Figure 3.3: Same as Figure 3.2 except that data sorted into forearc and backarc sites and only data having V_{s30} = 200–760 m s^{-1} are shown.

$(\mu_i)_{GMPE}$ = is the median value of that same IM from the GMPEs. Residuals in forearc and backarc regions are plotted versus distance in Figure 3.4 along with running means for distance bins. In forearc regions, the AEA 2012 residuals show a generally flat trend for distances up to approximately 150–200 km. At high frequencies, forearc residuals for all three GMPEs trend downward beyond approximately 150–200 km and then trend sharply upward beyond approximately 300 km. The sites producing the upward trend are principally on the south-east (forearc) side of Hokkaido. We do not know what feature of the crustal structure in this region might be responsible for this trend, although high Q (low crustal damping) has been noted in this region by Hashida (1987) [Has87]. The downward trends of high frequency forearc residuals for models AB and ZEA extend to close distances (approximately 50 km). At periods of 1.0 s and 3.0 s, the forearc residual trends are quite different among the three models, with AB trending strongly downward, AEA 2012 trending upward, and ZEA 2006 being relatively flat.

The backarc region, which begins at approximately 110 km, has high frequency residuals that trend downward to at least 300 km, especially for AB 2003 and ZEA 2006. This trend flattens or reverses beyond approximately 200 km (for AEA 2012) and 300 km (for AB 2003 and ZEA 2006). At longer periods, the backarc residuals follow generally similar trends to those in the forearc region, which is expected because the different anelastic attenuation of backarc regions has less effect for long period ground motion components. The general trends we have noted regarding the misfit of models to data at large distance is consistent with observations from prior studies (e.g., Furumura et al. 2011 [FTN11], Skarlatoudis and Papazachos 2012 [SP12], and Midorikawa et al. 2012 [MMA12]). The relatively strong distance attenuation in backarc regions has been noted previously by Ghofrani and Atkinson (2011) [GA11] and Skarlatoudis and Papazachos (2012) [SP12].

As shown in Figure 3.4, in most cases the data clouds are not centered at zero

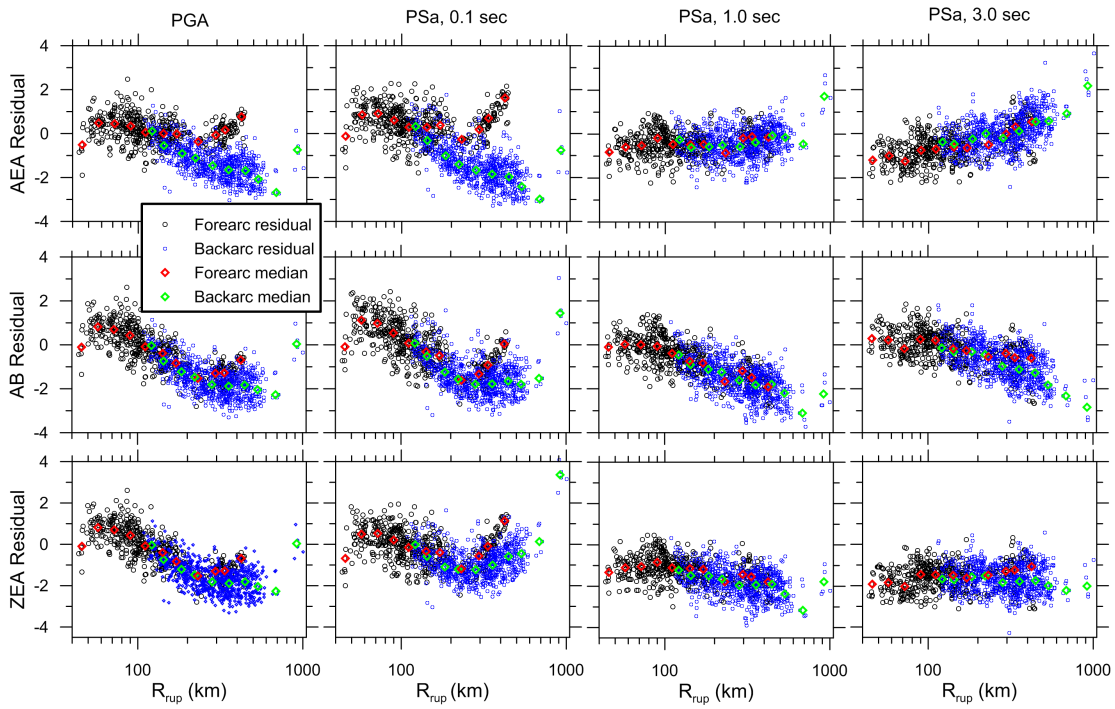

Figure 3.4: Total residuals of Tohoku-oki recordings within forearc and backarc regions relative to AB 2003, AEA 2012, and ZEA 2006 GMPEs along with mean residuals within distance bins.

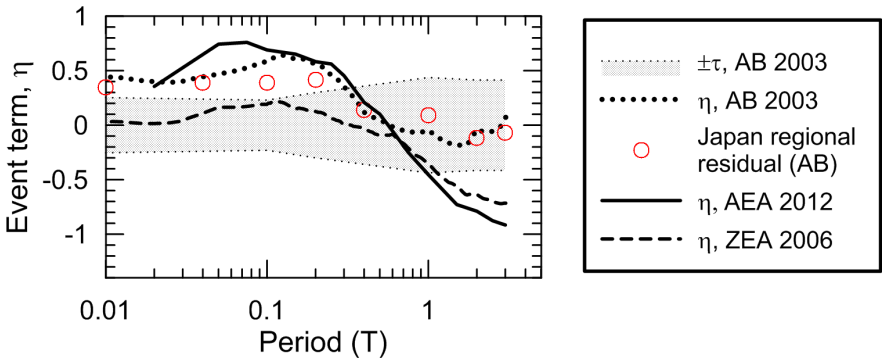

Figure 3.5: Estimated event terms of Tohoku-oki mainshock relative to the AB 2003, AEA 2012, and ZEA 2006 GMPEs. Also shown is the AB inter-event standard deviation (τ and the AB regional model bias for Japan (red circles). Estimated event terms were computed using data with $R_{rup} < 100\,\text{km}$.

ordinate, indicating systematic misfits of the GMPEs relative to the data. Since the event is very well recorded, this bias is practically equivalent to an event term as would be calculated from a mixed-effects regression (e.g., Abrahamson and Youngs, 1992 [AY92]). Non-zero event terms (η) are typical; what is of interest is to see if the Tohoku-oki event terms are consistent with event-to-event scatter (represented by event term dispersion τ) and regional trends of GMPE bias as observed from previous earthquakes. Figure 3.5 shows event terms, calculated as the median residual within 100 km, for the AB 2003, AEA 2012, and ZEA 2006 GMPEs as a function of spectral period along with the $\pm\tau$ model (inter-event standard deviation) from AB 2003. We only use residuals within 100 km because of the aforementioned distance attenuation misfits, which should not be mapped into event terms. The event terms peak at about 0.1 s and decrease at longer periods. The AB 2003 event terms follow closely the Japan region bias reported by AB 2003 (their Table 3), indicating that the misfit of the Tohoku-oki data relative to the AB 2003 model is consistent with previous data from Japan used in the development of the AB 2003 GMPE.

Event-specific intra-event standard deviations in natural log units (denoted as

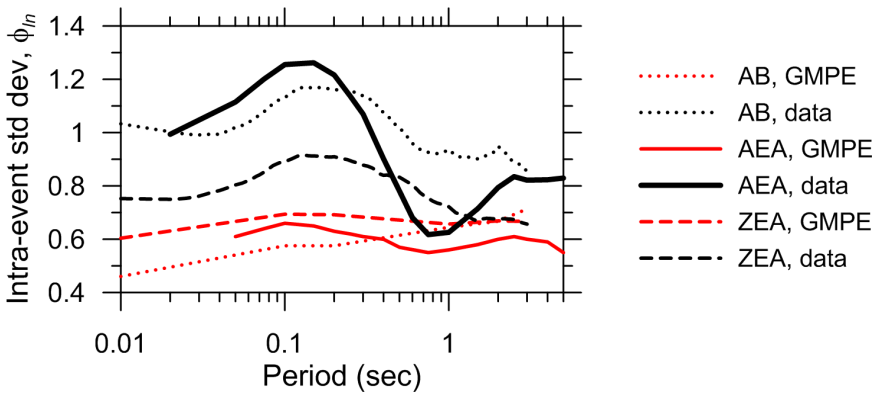

Figure 3.6: Intra-event standard deviation for Tohoku-oki earthquake data as compared to the AB 2003, AEA 2012, and ZEA 2006 intra-event standard deviations, ϕ_{ln}. Dispersion computed using data over all distances.

ϕ_{ln}) can be calculated as the standard deviation of residuals from Eq. (3.1). We compute this dispersion using residuals for all distances. Because the GMPE and data attenuation rates are significantly different, especially at short periods, the ϕ_{ln} values computed from data are higher than those from the GMPEs. Standard deviations for AEA 2012 and ZEA 2006 are substantially lower than those from AB 2003 at short periods due to more accurate distance attenuation. At long periods, dispersion levels for AEA 2012 and ZEA 2006 residuals fall to levels near those from the GMPEs.

3.4 Site effects

In this section, we present a preliminary evaluation of site amplification, specifically in reference to the scaling of ground motions with V_{s30}. As of this writing, we have not formally investigated higher-order effects such as nonlinearity in site response, which will be the subject of future work.

To evaluate site amplification, we utilize a non-reference site approach in which residuals are calculated between data and a GMPE applied for reference rock site

Table 3.1: Values of slope parameter c from analysis of reference rock residuals for forearcc sites with $R_{rup} < 200\,\text{km}$.

Slope parameter c	PGA	PSa, 0.1 s	PSa, 1.0 s	PSa, 3.0 s
AB	−0.053	0.273	−0.770	−0.732
AEA	−0.035	0.266	−0.642	−0.678
ZEA	−0.045	0.282	−0.767	−0.624

conditions as follows:

$$R_i^r = \ln\left(IM_i\right)_{rec} - \left(\ln\left(\mu_i^r\right)_{GMPE} + \eta\right) \tag{3.2}$$

where R_i^r indicates the residual of recording i from a rock GMPE, μ_i^r is a rock GMPE median for the magnitude and distance corresponding to recording i, and η is the event term appropriate for the earthquake event and IM. The reference site condition is taken as reference rock for AB 2003 (their site parameters S_C, S_D, and S_E are set to zero), $V_{s30} = 1100\,\text{m}\,\text{s}^{-1}$ for AEA 2012, and hard rock for ZEA 2006 (equivalent to NEHRP site category A).

A meaningful analysis of site effects from the Tohoku data set is complicated by the significant distance attenuation misfits identified in the previous section, which cause large non-zero residuals for reasons unrelated to site response. Accordingly, for the analysis of site effects, we use a subset of the data from forearc sites at rupture distances $R_{rup} < 200\,\text{km}$, for which distance attenuation trends are relatively well-matched by the GMPEs. Figure 3.7 shows the trends of AEA 2012 reference site residuals against V_{s30} for the intensity measures of PGA and PSa at 0.1 s, 1.0 s, and 3.0 s. A log-linear regression using all data is also shown along with its 95% confidence intervals. Table 3.1 shows the slopes of these fit lines (denoted as c) for the three models, which are similar.

The most important observation from the data trends in Figure 3.7 is the trend (or lack thereof) of reference site residuals with increasing V_{s30}. Low fre-

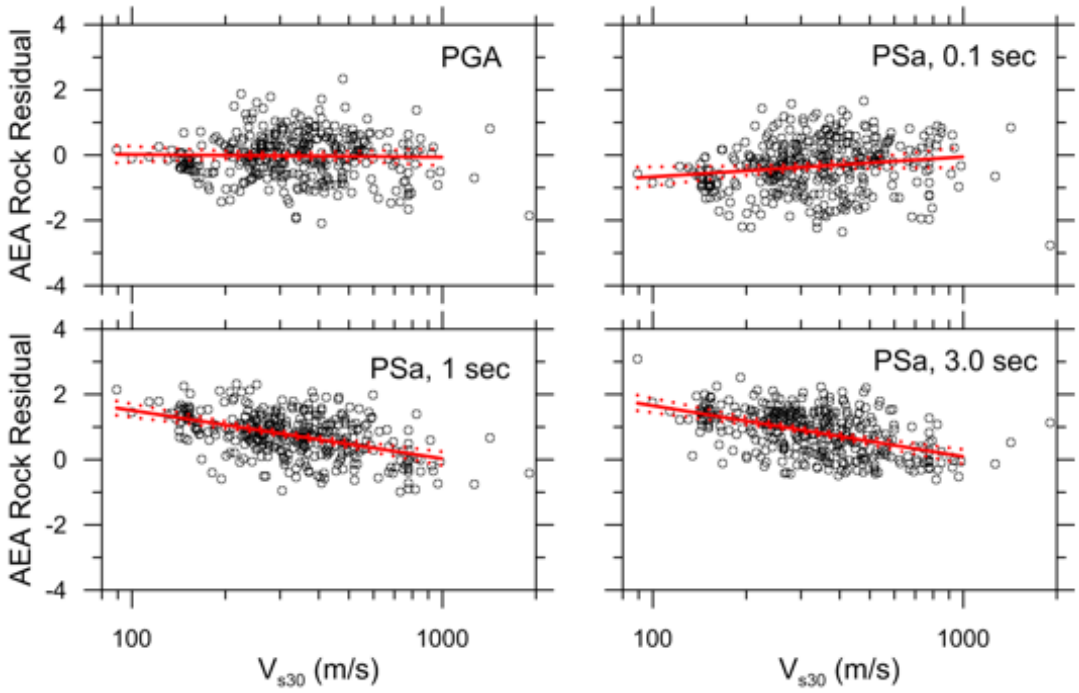

Figure 3.7: Reference rock residuals of Tohoku-oki recordings using AEA 2012 GMPE for rock site conditions. Residuals shown for forearc data with $R_{rup} < 200\,\text{km}$ along with linear regression fit and confidence intervals.

quency ground motions show a statistically significant trend as indicated by the negative slope of the fit line ($c < 0$), whereas high frequency ground motions have a relatively weak, or even positive, trend. These trends are different from those observed in most previous research, based largely on data from California (e.g., Borcherdt, 1994 [Bor94]; Choi and Stewart, 2005 [CS05]), which show significant trends with V_{s30} at low and high frequencies. This is a finding of considerable practical importance, as it suggests that the scaling of ground motions with V_{s30} is region-dependent. Regional variations in site response have been observed in previous research, although not (to our knowledge) in the form of regionally variable V_{s30}-scaling relationships. Atkinson and Casey (2003) [AC03] computed different site responses using quarter-wavelength theory for Japan and the Pacific Northwest, which explained regional differences in ground motions. Moreover, Oth et al. (2011) [OBP11] and Ghofrani et al. (2012, in press) [GAG12] have observed site response features in Japan, including significant high frequency amplification, which is seldom encountered in other active regions such as California.

We note that the data for high frequency IMs in Figure 3.7 show principally negative residuals between $V_{s30} \approx 130$ and $200\,\mathrm{m\,s^{-1}}$, which has been observed previously from Japanese data by the last author (KWC). It is not known whether this trend is sufficiently robust to support the use of a nonlinear V_{s30}-scaling relationship.

CHAPTER 4

Summary and Conclusions

The Tohoku-oki event is the largest magnitude earthquake to produce usable recordings. In combination with the data from the 2010 Maule, Chile, earthquake (Boroschek et al, 2012 [BCK12]), the data can be used to evaluate magnitude scaling of various ground motion intensity measures (IMs), which has generally been represented with linear or quadratic functions in recent GMPEs for subduction zone interface earthquakes. The data support saturation of the logarithm of IMs with increasing magnitude for the IMs considered, especially at high frequencies, indicating that linear magnitude scaling should not be used for large magnitudes.

The data demonstrate a scaling with distance that is demonstrably faster in backarc than forearc regions for high-frequency IMs. In both forearc and backarc regions, the AEA 2012 model best captures the high-frequency distance attenuation trends. All of the models under-predict the attenuation rate in backarc regions for high frequency IMs for rupture distances under about 200 km to 300 km. Distance attenuation misfits are mixed among the three models at long periods, being too-fast for AEA 2012, too-slow for AB 2003, and about right for ZEA 2006. The high-frequency distance attenuation trends are different from those from the Maule event (Boroschek et al., 2012 [BCK12]), where distance attenuation rates were slower and were well captured by the AB 2003 model and over-predicted by the ZEA 2006 model.

Using a non-reference site approach we find that the scaling of site amplification with V_{s30} is weak to non-existent for high frequency ground motions but strong

for low frequencies. Given the well-established and significant scaling of site amplification at low and high frequencies observed elsewhere (principally California), these findings suggest that the V_{s30} scaling of ground motions has regional dependence. This is not particularly surprising given that V_{s30} is a proxy for geologic structure, and since geologic conditions are regionally variable (e.g., Atkinson and Casey, 2003 [AC03]), the scaling of ground motion with V_{s30} can therefore also be expected to be region-dependent. Similar findings (unpublished) are also emerging from analysis of shallow crustal earthquake data in the NGA-West 2 project, indicating that this trend is not confined to this single earthquake.

We evaluate event terms using recordings within rupture distances of 100 km, because the problems with distance attenuation become particularly pronounced beyond that distance. Event terms are generally positive (indicating under prediction) for periods less than 0.7–1.0 s and peak at about 0.1–0.2 s. At periods longer than about 1.0 s the AB event terms are nearly zero, whereas AEA 2012 and ZEA 2000 event terms are negative. The AB 2003 event terms follow quite well the regional bias for Japan presented by AB 2003 with their Japan-specific regional correction factor.

Intra-event dispersion levels are higher than those from the corresponding GMPEs at high frequencies due to the distance attenuation misfits. The AEA 2012 and ZEA 2006 models have the lowest high-frequency dispersion levels among the three models. AB 2003 residuals have the highest dispersion due to the relatively large distance attenuation misfit. At long periods, dispersion levels from the AEA 2012 and ZEA 2006 models fall to levels near those from other GMPEs.

References

[AB03] GM Atkinson and DM Boore. "Empirical ground-motion relations for subduction-zone earthquakes and their application to Cascadia and other regions." *Bull. Seism. Soc. Am*, **93**:1703–1729, 2003.

[AB08] G.M. Atkinson and D.M. Boore. "Erratum to empirical ground-motion relations for subduction zone earthquakes and their application to Cascadia and other regions." *Bull. Seism. Soc. Am.*, **98**:2567–2569, 2008.

[AC03] B. Atkinson and R. Casey. "A comparative study of the 2001 Nisqually, Washington and Geiyo, Japan in-slab earthquakes." *Bull. Seism. Soc. Am.*, 2003. in press.

[AM09] G. Atkinson and M. Macias. "Predicted ground motions for great interface earthquakes in the Cascadia subduction zone." *Bull. Seismol. Soc. Am.*, **99**(3):1552–1578, 2009.

[ANA12] N. A. Abrahamson, Gregor N., and K. Addo. "C Hydro Ground Motion Prediction Equations for Subduction Earthquakes." *Earthquake Spectra*, 2012. submitted.

[AY92] N.A. Abrahamson and R.R. Youngs. "A stable algorithm for regression analyses using the random effects model." *Bull. Seism. Soc. Am.*, **82**:505–510, 1992.

[BB06] K. Beyer and J.J. Bommer. "Relationships between median values and between aleatory variabilities for different definitions of the horizontal component of motion." *Bull. Seism. Soc. Am.*, **96**:1512–1522, 2006.

[BCK12] R Boroschek, V Contreras, DY Kwak, and JP Stewart. "Strong ground motion attributes of the 2010 $M_w = 8.8$ Maule Chile Earthquake." *Earthquake Spectra*, **28**:S19–S38, 2012.

[Boo04] DM Boore. "Estimating V_{s30} (or NEHRP site classes) from shallow velocity models (depth $< 30\,\mathrm{m}$)." *Bull. Seism. Soc. Am.*, **94**:591–597, 2004.

[Boo10] D.M. Boore. "Orientation-independent, nongeometric-mean measures of seismic intensity from two horizontal components of motion." *Bull. Seism. Soc. Am.*, **100**:1830–1835, 2010.

[Bor94] R.D. Borcherdt. "Estimates of site-dependent response spectra for design (methodology and justification)." *Earthquake Spectra*, **10**:617–653, 1994.

[BTC11] DM Boore, EM Thompson, and H Cadet. "Regional correlations of V_{s30} and velocities averaged over depths less than and greater than 30 m." *Bull. Seism. Soc. Am.*, **101**:3046–3059, 2011.

[CDD08] BS-J Chiou, R Darragh, D Dregor, and WJ Silva. "NGA project strong-motion database." *Earthquake Spectra*, **24**:23–44, 2008.

[Cor68] C.A. Cornell. "Engineering Seismic Risk Analysis." *Bulletin of the Seismological Society of America*, **58**(6):1583–1606, 1968.

[CS05] Y. Choi and J.P. Stewart. "Nonlinear site amplification as function of 30 m shear wave velocity." *Earthquake Spectra*, **21**(1):1–30, 2005.

[DSG04] R Darragh, WJ Silva, and N Gregor. "Strong motion record processing for the PEER center." In *Proc. Workshop on Strong Motion Record Processing*, Richmond, CA, 2004.

[FTN11] T Furumura, S Takemura, S Noguchi, T Takemoto, T Maeda, K Iwai, and S Pdhy. "Strong ground motions from the 2011 off-the Pacific-Coast-of-Tohoku, Japan ($M_w = 9.0$) earthquake obtained from a dense nationwide seismic network." *Landslides*, **8**:333–338, 2011. Geological Survey of Japan, 1992. Geological Map of Japan.

[GA11] H. Ghofrani and G.M. Atkinson. "Forearc versus backarc attenuation of earthquake ground motion." *Bull. Seism. Soc. Am.*, **100**(5A):3032–3045, 2011.

[GAG12] H. Ghofran, G.M. Atkinson, and K. Goda. "Implications of the 2011 M 9.0 Tohoku Japan earthquake for the treatment of site effects in large earthquakes." *Bull. Eqk. Eng.*, 2012. in press.

[Has87] T. Hashida. "Determination of three-dimensional attenuation structure and source acceleration by inversion of seismic intensity data: Japanese islands." In *Bull. Earthquake Research Institute*, volume 62, pp. 247–287. University of Tokyo, 1987.

[MMA12] S Midorikawa, H Miura, and T Atsumi. "Strong ground motion during the 2011 Off the Pacific Coast of Tohoku earthquake." In *Proc. 9th Int. Conf. on Urban Earthquake Eng. & 4th Asia Conf. on Earthquake Eng.*, Tokyo, Japan, March 6–8 2012. Tokyo Institute of Technology.

[MWF06] M Matsuoka, K Wakamatsu, F Fujimoto, and S Midorikawa. "Average shear-wave velocity mapping using Japan engineering geomorphologic classification map." *Journal of Structural Mechanics and Earthquake Engineering*, **23**:57s–68s, 2006.

[OBP11] A. Oth, D. Bindi, S. Parolai, and D. Di Giacomo. "Spectral analysis of K-NET and KiK-net data in Japan, Part II: On attenuation characteristics, source spectra, and site response of borehole and surface stations." *Bull. Seism. Soc. Am.*, **101**:667–687, 2011.

[PCA08] M. Power, B. Chiou, N. Abrahamson, Y. Bozorgnia, T. Shantz, and C. Roblee. "An overview of the NGA Project." *Earthquake Spectra*, **24**:3–21, 2008.

[PFH08] M.D. Petersen, A.D. Frankel, S.C. Harmsen, C.S. Mueller, K.M. Haller, R.L. Wheeler, R.L. Wesson, Y. Zeng, O.S. Boyd, D.M. Perkins, N. Luco, E.H. Field, C.J. Wills, and K.S. Rukstales. "Documentation for the 2008 update of the United States national seismic hazard maps." In *Open-File Report 2008–1128*. US Geological Survey, 2008.

[RBP10] A Rodriguez-Marek, JA Bay, K Park, GA Montalva, A Cortez-Flores, J Wartman, and R Boroschek. "Engineering analysis of ground motion records from the 2001 Mw 8.4 Southern Peru Earthquake." *Earthquake Spectra*, **26**:499–524, 2010.

[SCS04] F Scherbaum, F Cotton, and P Smit. "On the use of response spectral reference data for the selection and ranking of ground motion models for seismic hazard analysis in regions of moderate seismicity: The case of rock motion." *Bull. Seism. Soc. Am.*, **94**:2164–2185, 2004.

[SM00] H. Si and S. Midorikawa. "New attenuation relations for peak ground acceleration and velocity considering effects of fault type and site condition." In *Proc. World Conf. Earthquake Eng.*, Auckland, NZ, 2000. Paper 0532.

[SMG13] JP Stewart, S Midorikawa, RW Graves, K Khodaverdi, H Miura, Y Bozorgnia, and KW Campbell. "Implications of Mw 9.0 Tohoku-oki Japan earthquake for ground motion scaling with source, path, and site parameters." *Earthquake Spectra*, **29**(S1), 2013.

[SP12] A Skarlatoudis and CB Papazachos. "Preliminary study of the strong ground motions of the Tohoku, Japan, earthquake of 11 March 2011: Assessing the influence of anelastic attenuation and rupture directivity." *Seism. Research Ltrs*, **83**:119–129, 2012.

[SSB09] G. Scasserra, J.P. Stewart, P. Bazzurro, G. Lanzo, and F. Mollaioli. "A comparison of NGA ground-motion prediction equations to Italian data." *Bull. Seism. Soc. Am.*, **99**(5):2961–2978, 2009.

[SSB12] J.P. Stewart, E. Seyhan, D.M. Boore, K.W. Campbell, M. Erdik, W.J. Silva, C. Di Alessandro, and Y. Bozorgnia. "Site effects in parametric ground motion models for the GEM-PEER global GMPEs project." In

15th World Conference on Earthquake Engineering. Lisbon, Portugal, September 2012.

[WM08] K Wakamatsu and M Matsuoka. "Development of national topography and site condition map with 250-m mesh size." In *Annual Meeting of Japan Association for Earthquake Engineering*, pp. 222–223. 2008. in Japanese.

[ZZA06] J.X. Zhao, J. Zhang, A. Asano, Y. Ohno, T. Oouchi, T. Takahashi, H. Ogawa, K. Irikura, H.K. Thio, P.G. Somerville, Y. Fukushima, and Y. Fukushima. "Attenuation relations of strong ground motion in Japan using site classification based on predominant period." *Bull. Seismol. Soc. Am.*, **96**:898–913, 2006.